Non-linear effects accompanying terawatt laser-pulse in air and their applications

Kamil Stelmaszczyk*[a], Philipp Rohwetter[a], Roland Ackermann[b], Guillaume Mjean[b], Jin Yu[b], Estelle Salmon[b], Jérôome Kasparian[b], Jean-Pierre Wolf[b], and Ludger Wöste[b]
1

[a]Institut für Experimentalphysik, Freie Universität Berlin, Arnimallee 14, D-14195 Berlin, Germany

[b]LASIM, Université Claude Bernard Lyon, 43 bd du 11 Novembre 1918, F-69622 Villeurbanne Cedex, France

ABSTRACT

Due to potential of applications, self-trapping of a peak-power laser pulse in a so called filament became an intensively investigated phenomenon. In this paper we demonstrate experimentally advantages of using filaments for the remote laser induced plasma spectroscopy (LIBS). This novel approach can increase effective range of conventional LIBS system up to single kilometers. We also show that Fourier-limited pulse does not optimize LIBS signal, opening the perspective for the pulse shaping techniques in a break-down spectroscopy.

Keywords: LIBS, filaments, femtosecond laser pulses, remote sensing

1. INTRODUCTION

Non-linear optical phenomena, like beam self-focusing[1] (SF), filamentation,[2] self-phase modulation[2] (SPM) and resulting supercontinuum (SC) generation,[3] induced in a transparent media by a powerful laser pulse have been subject of investigations for more then two decades. The early experiments could only be performed in solid or liquid phase, due to the moderate intensities of firs lasers. The development of the ultra-fast laser technology and especially chirp pulse amplification (CPA) technique[4], allowing generation of TW pulses with commercial products, laid foundations for the intensively growing interest in the non-linear effects and in particular filamentation induced in air.[5,6,7,8,9] Only shortly later, first experiment demonstrating a potential of practical applications of this phenomenon was performed.

In these first experiments a white light SC emitted from a filament was used for the broadband, range resolved absorption spectroscopy of the atmosphere[10] in visible and near-IR, reveling a clear signature of molecular H_2O and O_2. The vertical range reached 1 km with the spatial resolution of 250 m. For generating efficient SPM, 2TW, 100 fs (at optimum compression) pulses were used, which were subsequently chirped negatively (opposite to air dispersion) to compensate GVD in air. In this way the starting point of the SC emission relative to laser position could be controlled, because the pre-chirped pulse undergoes a self-shortening leading to the increase of its intensity during the propagation.

There are, however, much more properties of filaments interesting form practical point of view.[11] For example, a highly collimated, stable propagation mode, which- as it will be explained in details in a next section- results from quasi-equilibrium between Kerr self-focusing and beam self-focusing due to air ionization. This mode is additionally stabilized by the fact that the refractive index inside the filament is modified by an amount exceeding air thermal and density fluctuations, typically $\Delta n \sim 10^{-5}$. Relatively large change of refractive index together with a high free electron density makes filament almost insensitive to external conditions. As a consequence, the longitudinal extent of a filament exceeds many times beam's Rayleigh length.[12,13] Moreover, kilometer-range propagation distances of filaments have been reported.[14]

* kamil.stelmaszczyk@physik.fu-berlin.de, tel. +49 30 838 56119, fax +49 30 838 53444

The ability of filaments to overcome the diffraction limit and to deliver high light intensities over kilometer distances makes them ideal light sources for long-distance remote laser induced breakdown spectroscopy (LIBS). In this technique a laser pulse is focused on a sample surface leading to plasma generation. Successive detection of atomic and ionic emission allows for material chemical composition analysis. In LIBS no special preparation of the material surface is needed. The only requirement is the sample accessibility for the laser light. For this reason, LIBS can also be adopted for stand-off or remote sensing applications, provided that the laser intensity is above the material ablation threshold. This requirement can easily be met for distances of several meters, using focusing optics.[15] For longer distances, the use of sophisticated long focal-length systems or a lens right in front of the target is unavoidable.[16] Even with this approach the distances up to few dozens of meters are only available. Beyond this limit prohibitively large beam expanders become indispensable.

In this paper we report on the LIBS experiments, which for the first time were based on the filamentation. With this novel approach the plasma was be generated at distances as long as 180 m. We also present the comparison of the laser ablation using femto-, pico- and nanosecond pulses.

2. FILAMENTATION

Incase of a high intensity laser pulse, air response to the varying electric field $\boldsymbol{E}$, which is usually described in terms of macroscopic polarization $\boldsymbol{P}$, becomes non-linear:[17]

$$\boldsymbol{P} = \varepsilon_0 \chi_{eff} \boldsymbol{E} = \varepsilon_0 (\chi^{(1)} + \chi^{(2)} \boldsymbol{E} + \chi^{(3)} \boldsymbol{E}\boldsymbol{E} + ...) \boldsymbol{E} . \quad (1)$$

In above equation ε_0 is the vacuum permittivity and $\chi^{(i)}$ describe respective order electric susceptibility. Due to air isotropy the relation:

$$\boldsymbol{P}(\boldsymbol{E}) = -\boldsymbol{P}(\boldsymbol{E}) \quad (2)$$

must be fulfilled, meaning that all non-linear terms including even orders susceptibilities must be equal to zero. In such a case and when taking into account terms not higher then the third order Eq. (1) can be rewritten in a simplified form:

$$\boldsymbol{P} = \varepsilon_0 \chi_{eff} \boldsymbol{E} = \varepsilon_0 (\chi^{(1)} + \chi^{(3)} \boldsymbol{E}\boldsymbol{E}) \boldsymbol{E} . \quad (3)$$

Eq. (3) imposes that the dielectric function of air-$\varepsilon_{non\text{-}linear}$- is changed by the presence of the intense laser pulse, namely:

$$\varepsilon_{non-linear} = \varepsilon_0 (1 + \chi^{(1)} + \chi^{(3)} E^2) . \quad (4)$$

Given Eq. (4) the modified air refractive index can be expressed in terms of the formula:

$$n_{non-linear} = n_0 + n_2 I , \quad (5)$$

in which the light pulse intensity, proportional to the square of the electric field vector, was denoted by I. The $n_0 = 1 + \chi^{(1)}$ and $n_2 = \chi^{(3)}/(n_0 \varepsilon c)$, where c is the speed of light in vacuum, correspond to the linear and non-linear refractive index of air, respectively. Eq. (5) is valid not only for air but also any other isotropic medium and reflects its tendency to become optically thicker under illumination by intense light pulse. Such an effect is well known as a Kerr effect.

For Gaussian or semi-Gaussian beam, Kerr effect will act against the beam diffraction. Above a certain threshold Kerr effect can overcome diffraction and SF will occur. Provided that the non-linear refracting index of the medium is known the, critical power P_{crit}, *i.e.* the power needed for starting the beam SF, can be estimated by the formula:

$$P_{crit} = \frac{\lambda^2}{2\pi n_0 n_2} . \quad (6)$$

For air and laser wavelength λ=800 nm, n_2=3.0·10^{-19} cm^2/W,[18] meaning that for commonly used Ti:Sapphire P_{crit}≅3 GW.

The intensity inside the self-focusing beam continuously increases. At certain position plasma generation will occur. Because typical collision time in air is in order of single picoseconds,[19] the processes of collision ionization can be neglected, for short femtosecond pulses. Plasma is then created by Tunnel Ionization (TI) or Multi-Photon Ionization (MPI). Because the ionization potential of main air constituents: nitrogen and oxygen are respectively 15.6 eV and 12,1 eV, at least few photons (depending on the wavelength) are involved in the ionization. For λ=800 nm the number of photons are eight for the oxygen and eleven for nitrogen. MPI is dominant for intensities 10^{13}-10^{14} W/cm^2. Above this threshold TI becomes more probable.[19]

The electron density at a given position inside the focusing beam is given by the rate equation[20]:

$$\frac{\partial \rho_e(t)}{\partial t} = R(I)[N_0 - \rho_e(t)], \tag{7}$$

where ρ_e is the free electron density, N_0 is the initial density of neutral molecules and $R(I)$ is the ionization rate dependent on the laser intensity. The ionization rate is the power function of the laser intensity. Assuming plasma generation by pure MPI the power index corresponds to multi-photon process order. This reflects the fact that probability of a n-photon absorption is proportional to I^n. However, for filamentation the effective index power is lower then that resulting from the ionization potential. It is due to additional contribution of TI. For example, Kasparian *et al.*[21] estimated n=7.5 and n=6.5 for nitrogen and oxygen ionization, respectively.

Plasma contribution to air dielectric function is negative. It is usually expressed in terms of plasma frequency:[22]

$$\omega_p = \sqrt{\frac{\rho_e e^2}{m\varepsilon}}, \tag{8}$$

where ρ_e is a free electron density, e -electron charge and m corresponds to an electron mass. Using the plasma frequency the dielectric function of air in the presence of free electrons can be determined. Because the self-focusing volume of air is modified by Kerr effect, the dielectric function must be represented by the formula:

$$\varepsilon_{air} = \varepsilon_{non-linear}\left(1 - \frac{{\omega_p}^2}{\omega^2}\right), \tag{9}$$

where $\varepsilon_{non-linear}$ represents the non-linear dielectric function and ω denotes the laser frequency. Combining Eq. (8) and Eq. (9) leads to:

$$\varepsilon_{air} = \varepsilon_{non-linear}\left(1 - \frac{\rho_e}{\rho_{crit}}\right), \tag{9}$$

where ρ_{crit} defines the electron density, for which the plasma frequency is equal to the laser frequency. For λ=800 nm the critical electron density ρ_{crit}=1.75 10^{21} cm^{-3}. This value is relatively large in comparison with typical atmospheric density ρ_{air}=2.46 10^{19} cm^{-3} (for standard temperature and pressure conditions: 298 K and 1013 hPa, respectively). Thus, the refracting index of air in the presence of plasma electrons can be calculated with the assumption ρ_{crit}>>ρ_e:

$$n_{air} = \sqrt{\frac{\varepsilon_{air}}{\varepsilon_0}\left(1 - \frac{\rho_e}{\rho_{crit}}\right)} \simeq n_{non-linear} - \frac{\rho_e}{2\rho_{crit}}. \tag{10}$$

According to the rate equation (Eq. (7)) the ionization in the central part of the beam is the higher than on the edges. Such a distribution forms a "negative lens" and defocusing begins. This effect is opposite to the Kerr self-focusing. Taking into account both Kerr and plasma contribution the effective refractive index of air n_{air} can be expressed in a form:

$$n_{air} = n_0 + n_2 I - \frac{\rho_e(I)}{2\rho_{crit}}. \tag{11}$$

In the above equation the dependence of ρ_e on intensity was explicitly indicated.

The propagation equation with modified refractive index is strongly non-linear and its solution turns out to be extremely sensitive to initial conditions. For example, a slight modification of beam diameter or pulse duration can result in self-collapsing or stable propagation mode. In general, however, three distinctive regions of propagation can be distinguished.[23] In each of them the beam cross-section evolution is governed by the actual intensity. At first, the beam diameter undergoes a gradual transverse suppression initiated by Kerr effect. No plasma generation is present in this region. The spectral and temporal characteristic remains practically unchanged and only weak contribution of self-phase modulation can be observed. Near the focal point of a Kerr lens the filed amplitude undergoes rapid increase. This gives rise to many accompanying effects including pulse self-shortening, MPI, or SC emission. Plasma inside the focus retards Kerr effect and a dynamical equilibrium between self-focusing and plasma defocusing occurs. Consecutive convergence and divergence guides the energy in a stable filament, which is clearly distinguished from the rest of the beam. Filament is, therefore, treated as an autonomous propagation mode.[24] The incidence of filamentation defines the third region of propagation.

The mechanism presented above is still under discussion.[25] It explains qualitatively the process of filamentation in the framework of so called spatial replenishment model.[26] The spatial replenishment model is valid only if the pulse power is equal to or slightly higher then P_{crit}. A single filament is formed in such a case and its position is always near to the intensity maximum. With a power increased significantly above P_{crit} a phenomenon of multiple filamentation takes place.[27] In the multiple filamentation filaments become randomly arranged with their position determined by the small-scale power fluctuations. This random fluctuations act as a micro Kerr cells with the power close to P_{crit}.[28] The number of cells and consequently resultant filaments cannot be, however, estimated by simple multiplicity of P_{crit}. For example, if the pulse power is several hundred times greater then the critical power, typically as few as 20-30 filaments are formed inside the beam (Fig. 1).

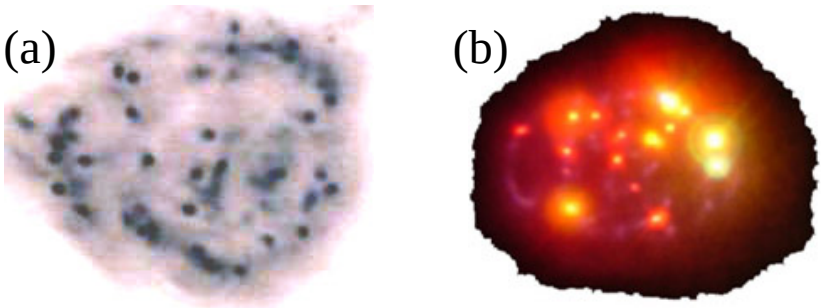

Figure 1. Fialmentation: (a) beam impact with a burn-paper, (b) picture taken with a digital camera. In both cases 20-30 plasma channels are visible. Emission of white-light from filaments is due to SPM and plasma.

Filaments created in air through single or multiple filamentation are very similar. Their diameter is variable in a small range between 70-100 μm.[29] Light intensity inside a filament varies between 10^{13}-10^{14} W/cm^2.[30] This order of magnitude is mainly set by the MPI. A high intensity induces modifications of air refractive index by the factor of

10^{-6}-10^{-5}, sufficiently enough to overcome atmospheric thermal and density turbulence. Efficient self-phase modulation inside a filament generates a spectrally broad SC[31] partially emitted in a form of conical emission.[32] The free electron density inside the filament[33] ρ_e ~10^{16}-10^{17} cm^{-3}, which is only two orders of magnitude smaller that the air density. It is worth to note that UV filaments are much different from the one formed in IR. In UV filaments the electron density and average peak-intensity are few orders of magnitude lower, while the diameter is only slightly increased.[34] This difference is explained by lower intensity threshold for MPI in UV (higher energy of photons means lower number of photons absorbed).

3. EXPERIMENTAL SETUP

In experiments we used filaments generated by a mobile femtosecond laser- Teramobile. Teramobile is a terawatt-class laser system together with detection unit integrated in standard ISO container. A detailed description of the device can be found elsewhere[35] and only a brief summary will be given here. The laser is based on the Ti:Saphire seeder, delivering ~nJ, 70 fs pulses of 795 nm wavelength and a CPA amplifier. Before amplification pulse duration is increased to 200 ps. It is necessary due to the high 10^8 amplification factor of the system and puts the power below the damage threshold of optical elements. Three amplification stages are present. At first, pulses are sent into a regenerative amplifier. Its confocal design assures stable beam profile crucial for a homogeneous amplification in multipass amplifiers. After regenerative amplifier pulses pass through the first multipass amplifier in which their energy is increased to 40 mJ. From

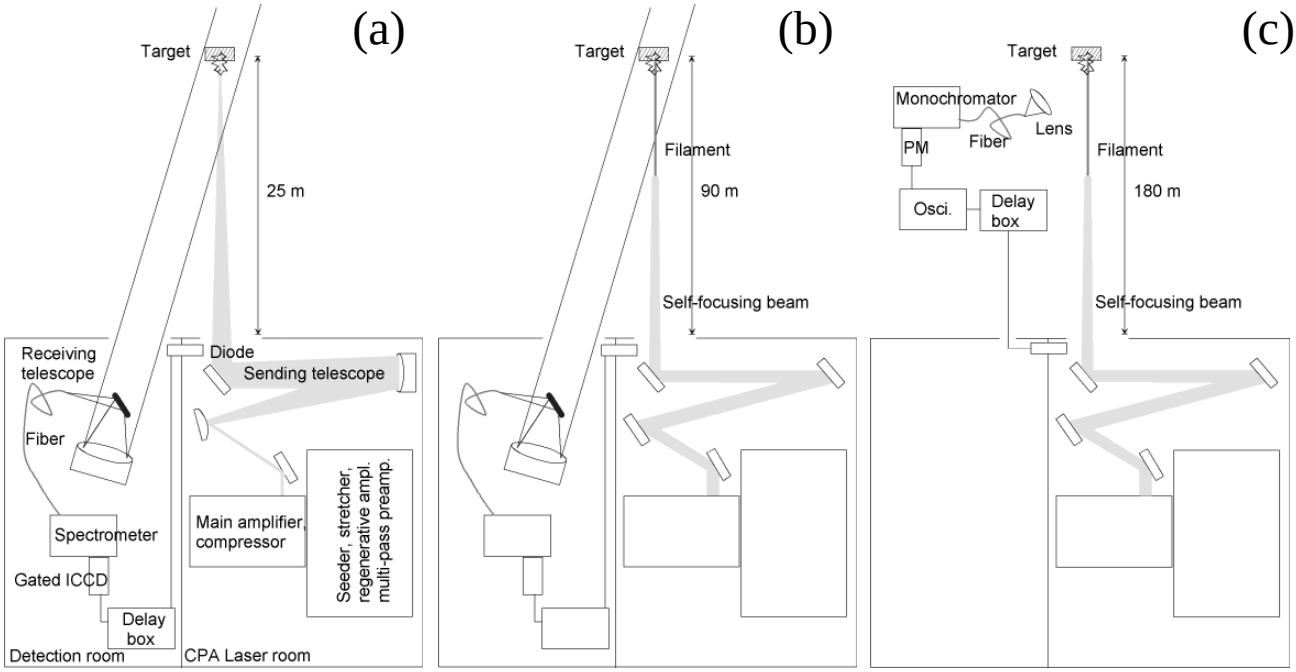

Figure 2. (a) Focused beam geometry with the detection based on the ICCD camera. This configuration was used with the target located 25 m from the container. (b) The collimated beam geometry for the target positioned at the distance of 90 m. In this configuration plasam could only be induced by filaments due to large 5 cm diameter of the beam. (c) The collimated beam geometry combined with the detection based on the monochromator and photomultiplier. The distance between the laser and the target was 180 m. The distance between the lens and the target was 1.5 m.

this level the final amplification in a main amplifier takes place. The pulse energy after the main amplifier is typically 400-500 mJ, but can be reduced by turning the one of the half-wavelength plates. The beam diameter is subsequently expanded to 5 cm and the pulse recompression in the grating compressor takes place. The pulse duration can be continuously adjusted in the range between ~70 fs - ~1 ps. The shortest duration corresponds to nearly Fourier-limited pulse. By by-passing the compressor the pulses of 200 ps can be obtained; with the unseeded regenerative amplifier 5 ns pulses. The beam is sent outside as focused or collimated. In the experiments both beam geometries were used: focused at short and collimated at long distances.

On the detection side we used an f=500 mm, F5 Newtonian telescope (or f=800 mm, F4) and f=500 mm, F8 Czerny-Turner spectrometer (Chromex 500 IS/SM). For coupling a fiber bundle with F-number adapter was applied. As a detector an ICCD camera (Stanford PI MAX 1024HQ) in the spectrometer's reciprocal plane was used. The camera was triggered with a selectable delay by photododiode, pointing to the laser pulse at the beam output. In such a configuration the delay had to be adjusted each time we changed the distance to the sample. In a configuration described above the maximal detection distance was 150 m. Visual observation of the filament plasma on the target suggested, however, that the poor detection sensitivity, rather then filament strength was the main factor limiting measurement range. Indeed, the low spectral efficiency of the diffraction grating and as many as five reflections from coated aluminum mirrors inside the Czerny-Turner spectrometer resulted in the overall transmittance of the receiver setup ~14%.[36] To avoid this problem second detection was used. This time the plasma light was focused directly on the fiber input, using the f=250 mm, 50 mm diameter lens. The lens was located 1.5 m in front of the target. The fiber output was directly connected to the input slit of f=250 mm, F5 grating spectrometer (Oriel MS257). Instead of the ICCD camera, the photomultiplier (Hamamatsu 6780-03) was attached to the exit slit of the spectrometer. The signal from the photomultiplier was recorded by the digital oscilloscope (LeCroy Waverunner LT334). In Fig. 2 the differences in the experiment geometry, as well as detection are presented.

4. EXPERIMENTAL RESULTS AT 25 m

To demonstrate a difference in LIBS signals induced by femto-, picosecond pulses copper and aluminum samples were positioned in front of the laser at 25 m distance. The spectra were recorded in focused beam geometry (Fig. 2(a)). The entrance slit of a spectrometer was 100 μm and a reflection grating with 600 lines/mm was selected. This combination corresponded to the theoretical resolution of 0.34 nm. Despite different durations: 75 fs, 200 ps and 5 ns the pulse energy was always comparable. In the first case 205 mJ and in the second and third case 220 mJ measured at the beam output. Since pulse energies were similar, characteristic features of emitting plasma must be attributed to the representative time scale of the laser-sample interaction.

In Fig. 3 recorded spectra from copper near 800 nm are depicted. Fig 3(a) presents the result of ablation with fs pulses. In this case the camera was triggered 10 ns after arrival of SC light reflected from the target with a gate of 10 μs. The spectrum was averaged over 400 shots. In case of Fig. 3(b) picosecond pulses were used. With longer pulses light intensity turned out to be much higher and averaging over only 30 shots was introduced. The gate was reduced to 1 μs and delay was increased to 400 ns. Relatively long, microsecond gating time for all pulse durations matched fluorescence decay, which was much longer than to previously reported in low fluence regime.[37] First two spectra (Fig. 3(a)-(b) correspond to the sample embedded in atmospheric air. For the spectrum from Fig. 4, a constant flow of Ar was additionally delivered near the sample.

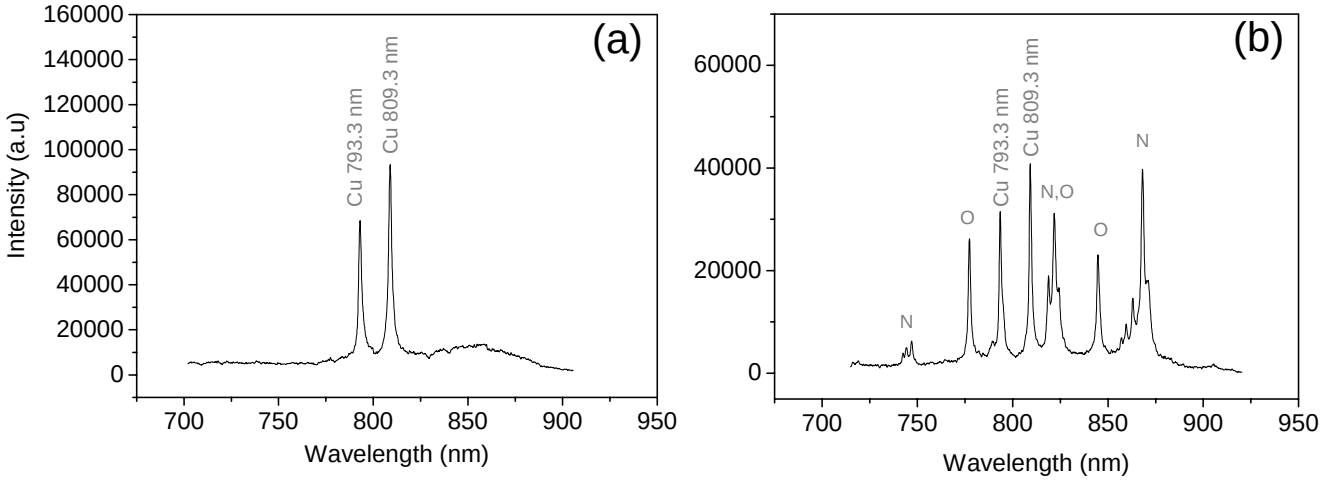

Figure 3. Copper emission near 800 nm, (a) ablation with 75 fs femtosecond pulses (b) ablation with 200 ps pulses. For both figures the sample the ambient gas was atmospheric air.

Even after a brief comparison of spectra from Fig. 3(a)-(c) it becomes evident, that the ablation in the femtosecond time scale is qualitatively different than the one with longer pulses. Namely, no interfering emission from the ambient gas is present in femtosecond case. Using picosecond pulses, additional lines can be related to atmospheric oxygen and nitrogen. For the last spectrum primary air constituents' emission is accompanied by supplementary Ar lines. Similar observation can be done after replacing copper by aluminum.[38]

The lack of ambient gas emission in femtosecond spectra suggests two different ablation mechanisms in ultra short and longer time scale. Since the femtosecond interaction time is much shorter than the relaxation of lattice-electrons, direct contact between light and ejected material vapor cannot take place. The thermal equilibrium is, therefore, established without the pulse. Consequently, only a low temperature and local plasma is formed and the excitation in the ambient gas becomes negligible. The mechanism of laser ablation with longer pulses is different. At the early-stage a jet of highly energetic electrons is formed. The electrons expand in the direction perpendicular to the surface at the velocity of 10^9 cm/s and ionize surrounding medium by collisions.[39] The electronic jet is then followed by the hot plume of removed material. This plume expands at the much lower velocity (10^6 cm/s) and absorbs the incident laser energy. Eventually, it further ionizes the ambient gas leading to its enhanced emission. The conversion of pulse energy into the forming plasma thermal energy is much more efficient, in this case. We note here, that direct ionization of the air near the sample was not possible in our experiments due to low pulse intensity, approximately 10^9 W/cm^2 and 10^7 W/cm^2 for picosecond and nanosecond pulses, respectively.

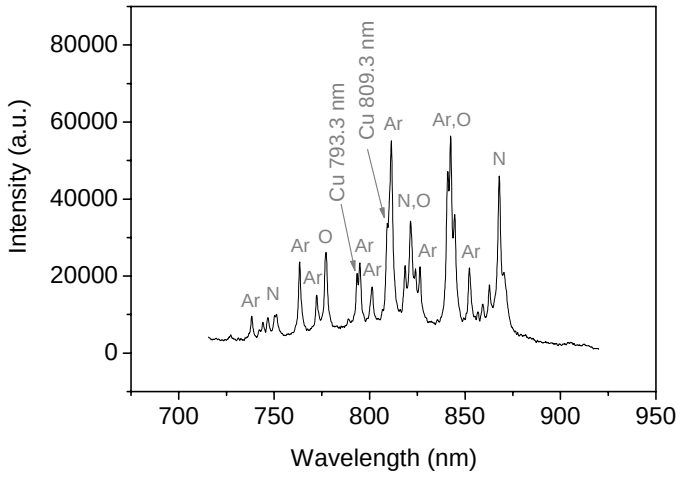

Figure 4. Copper emission near 800 nm. Ablation with 200 ps pulses in a constant flow of Ar.

The model of plasma heating by the pulse tailing part is insufficient to explain the dependence of the line intensity on the laser pulse chirp. The dependence of this type was clearly confirmed in our next experiment. The pulse energy was increased to 250 mJ. Emission from the copper around 520 nm was measured as a function of chirp applied to the laser pulse. The pulse duration varied between 70 fs and about 0.4 ps with both positive (longer wavelengths first) and negative (shorter wavelengths first) chirps. The camera was gated with 500 ns delay and 10 μs gate. The result for Cu 521.8 nm line is presented in Fig. 5.

Intensity changes are much better pronounced for a negative chirp with the tendency of lower signal with shorter pulses. Signal amplitude variations with positive chirp are smaller. Almost constant emission from the samples was measured in the applied pulse duration range. A clear asymmetry between both parts of curves (negative and positive chirp) is evident. This asymmetry suggests that apart from pulse duration the spectro-temporal pulse characteristic plays an important role in the plasma formation.

The influence of pulse chirp on fluorescence intensity was previously observed in rubidium vapors.[40] Similar observations were reported also for dye molecules with the shaped laser pulses.[41] Since experiments in the gas phase confirmed the possibility coherent population transfer control for very complex dye molecules, observed effect may suggests the perspective for the pulse-shaping LIBS. Our result must be, however, considered as a preliminary, because it

includes the uncertainty of the compressor calibration. Moreover, in the classical pulse-shaping the fluorescence modulation is explained by the interference between phase-shifted resonant and off-resonance transitions in the two-photon (or in general multi-photon) ladder climbing. This relatively easy description is not applicable to the laser ablation, which is much more complicated process. Plasma generation involves several interacting stages, starting from electronic excitation to photoelectric and thermal processes.[42] In such a case, the theoretical description from the gas phase cannot be directly valid. For this reason new theoretical models, combined with extended experimental work are necessary to confirm and satisfactory explain observed phenomenon

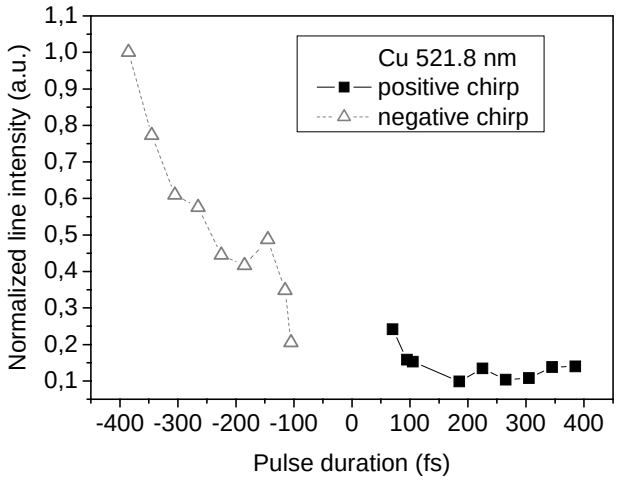

Figure 5. Normalized emission intensity of Cu (521.8 nm) as a function of pulse chirp. The shortest pulse was arbitrary classified as positively chirped. The asymmetry in emission between negative (shorter wavelengths in a pulse leading part) and positive (longer wavelengths in a pulse leading part) chirps cannot be explained by simple pulse duration.

5. EXPERIMENTAL RESULTS AT 90 m

With a sample positioned at 90 m from the laser container the experiment configuration from Fig. 2 (b) was used. This choice was dictated by the simple fact that spherical aberrations together with beam divergence reduce a delivery of high intensities at long distances. But inside collimated TW beam filaments are formed. The only requirement is then to apply appropriate pulse chirp, which controls the distance of filamentation. The onset material ablation induced by filaments enables long distance remote LIBS. We call this new approach remote FIBS (Filament Induced Breakdown Spectroscopy).[43]

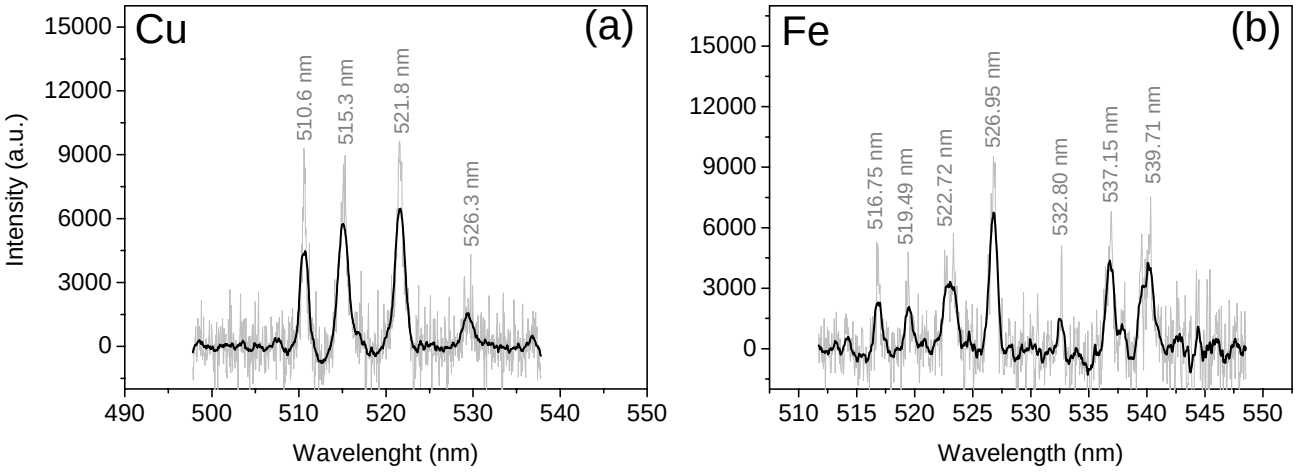

Figure 6 FIBS spectra of Cu and Fe spectrum detected remotely from 90 m. No beam focusing was applied.

Fig. 6 presents the FIBS spectra of Cu (Fig 6(a)) and Fe (Fig. 6(b)). As previously long 10 μs camera gate with shorter 10 ns delay was used. The pulse initial negative chirp was set to 380 fs. This corresponded to 289 fs pulses near the sample, assuming pulse recompression with group velocity dispersion in air 1.01 fs/m[44]. The spectra were averaged over 10 000 shots, to assure high signal-to-noise ratio, however, unquestionable signature of the metal fluorescence could be confirmed with as little as 1000 shots. Surprisingly, the measurement of the FIBS signal as a function of distance R revealed only geometric optics $1/R^2$ (Fig. 7). Such a behavior is in a strong contrast with the standard LIBS, when focused beam waist increases proportional to the distance.[45] Since plasma generation is strongly non-linear process, the intensity decrease is not fully balanced by the increase in the illuminated area. Consequently, the signal decrease faster then $1/R^2$ is observed. In this perspective, slower attenuation of the FIBS signal can be helpful in increasing the effective range of LIBS systems; possibly to the single kilometers.

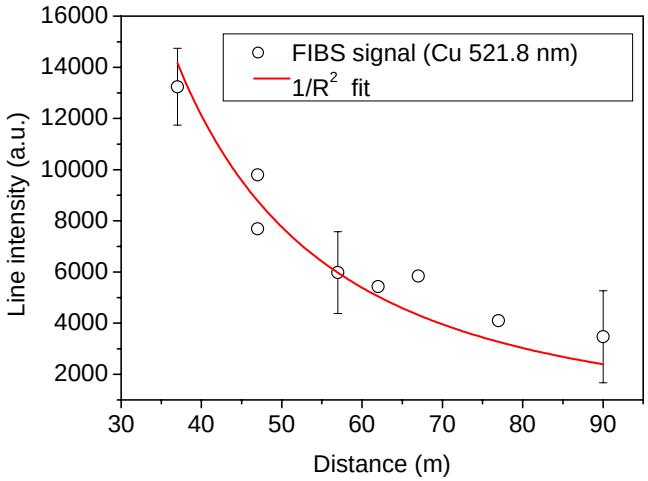

Figure 7. Intensity of Cu 521.8 nm line as a function of distance to the target. FIBS signal proportional to $1/R^2$ proves that filaments can overcome diffraction limit of focused beam.

6. EXPERIMENTAL RESULTS AT 180 m

The success of remote kilometer LIBS can only be attained, providing light sources capable to induce plasma at these distances. To demonstrate, that filaments seem to be an ideal choice for this task we measured emission from aluminum plasma at 180 m. A detection based on the monochromator and photomultiplier connected to the digital oscilloscope was used. With this setup a temporal evolution of fluorescence could be measured in a straightforward manner and no temporal gating with shifted delay is necessary. A special attention must be, however, paid to avoid strong SC light reflected from the target. To avoid PM's non-linear response two UV (394,4 and 396,1 nm) emission lines of Al were chosen. As it is well known, a spectral intensity of the SC in UV is few orders of magnitude lower then in visible.[46]

The spectrum obtained by a wavelength scan is presented in Fig. 7(a). Its low resolution results from the convolution with a wide 1 mm output slit. Despite low resolution, the line contrast is very high and the presence of two emission peaks is unambiguous. The fluorescence lifetime (Fig. 7(b)) is about 120 ns, corresponding well to previous investigations in a low fluence regime (1 mJ, 140 fs). Indeed, the energy accumulated in a filament is typically 1 mJ, which is only a small fraction of the total pulse energy.

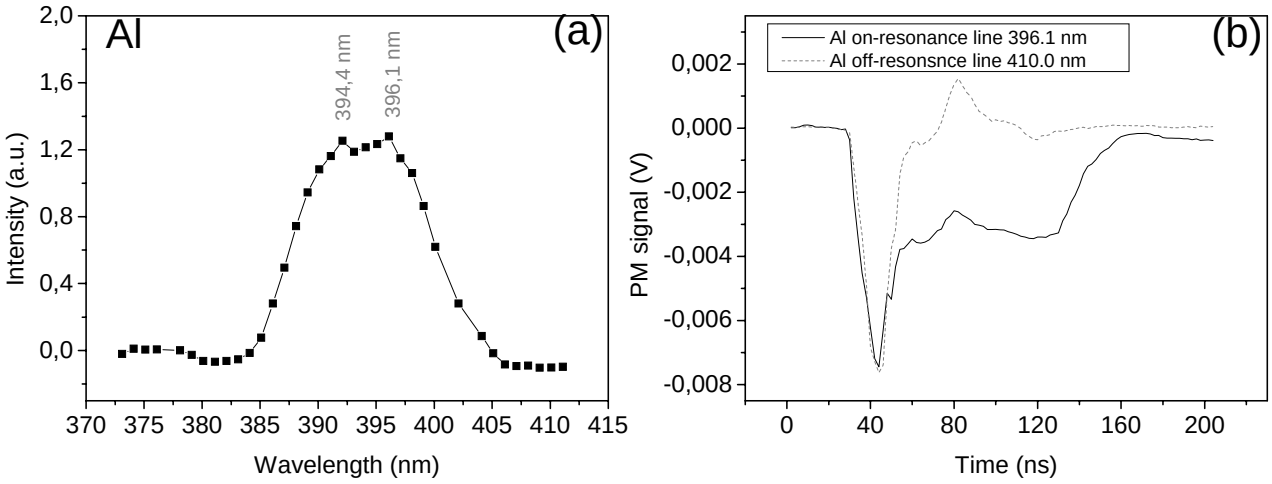

Figure 7. (a) Al spectrum from plasma induced by filaments at 180 m measured by monochromator wavelength scan, (b) fluorescence life time; peak at 40 ns defines zero time and includes also SC light.

7. CONCLUSION

Using a container integrated femtosecond laser system Teramobile we performed systematical analysis of the LIBS signal induced by laser pulses of durations in femto-, pico- and nanosecond time scale as well as filaments. With longer pulses (nano- and picosecond) a strong interference from the ambient gas was observed. With the femtosecond and filament ablation the occurrence of additional emission imposed on metal fluorescence could not be identified. Similar results were obtained in a natural atmospheric and argon environment, with three different samples made of industrial grade aluminum, copper and iron, proving low sensitivity of the femto-LIBS to the overlapping emission from the material under investigation and surrounding gas. A detailed investigation of the fluorescence revealed clear non-linear features manifested by the signal dependence on the applied chirp and not only the pulse duration. This observation opens perspectives for the pulse-shaping LIBS. The ability of the laser to generate pulse of a power exceeding many times the critical power for beam filamentation allowed us to demonstrate for the first time remote Filament Induced Breakdown Spectroscopy (R-FIBS). With filaments the diffraction limit of the focused beam can be overcame and the plasma can be generated on targets at distant locations. We demonstrated this ability up to the 180 m, opening perspective for long distance remote LIBS.

ACKNOWLEDGMENTS

This work has been performed within the framework of the Teramobile project, jointly funded by the French CNRS and the German DFG. Kamil Stelmaszczyk acknowledges fellowship of the Alexander von Humboldt Foundation.

REFERENCES

1. J. H. Marburger, “Self-focusing: Theory”, Prog. in Quantum Electron. **4**, 1-110, 1975
2. R. R. Alfano, S. L. Shapiro, “Observation of self-phase modulation and small-scale filaments in crystals and glasses”, Phys. Rev. Lett. **24**, 592-594, 1970
3. P.B. Corkum, P.P. Ho, R.R. Alfano, J.T. Manassah, “Generation of Infrared Supercontinuum Covering 3-14 Mum in Dielectrics and Semiconductors”, Opt. Lett. **10**, 624-626, 1985
4. A. Antonetti, F. Blasco, J.P. Chambaret, G. Cheriaux, G. Darpentigny, C. Le Blanc, P. Rousseau, S. Ranc, G. Rey, F. Salin, “A laser system producing 5×10^{19}W/cm^2 at 10Hz”, App. Phys. B, **65**, 197-204, 1997

5. A. Braun, G. Korn, X. Liu, D. Du, J. Squier, G. Mourou, “Self-channeling of High-peak-power Femtosecond Laser Pulses in Air”, Opt. Lett. **20**, 73-75, 1995
6. O. G. Kosareva, V. P. Kandidov, A. Brodeur, C. Y. Chien, and S. L. Chin, “Conical emission from laser-plasma interactions in the filamentation of powerfull ultrashort laser pulses in air”, Opt. Lett. **22**, 1332-1334, 1997
7. L. Wöste, C. Wedekind, H. Wille, P. Rairoux, B. Stein, S. Nikolov, C. Werner, S. Niedermeier, F. Ronneberger, H. Schillinger and R. Sauerbrey, “Femtosecond atmospheric lamp”, Laser und Optoelectronik **29**, 51-53, 1997
8. S. Tzortzakis, M.A. Franco, Y.B. Andre, A. Chiron, B. Lamouroux, B.S. Prade, A. Mysyrowicz, “Formation of a conducting channel in air by self-guided femtosecond laser pulses”, Phys. Rev. E **60**, R3505-R3507, 1999
9. S.L. Chin, S. Petit, W. Liu, A. Iwasaki, M.-C. Nadeau, V.P. Kandidov, O.G. Kosareva, K.Yu. Andrianov, “Interference of transverse rings in multifilamentation of powerful femtosecond laser pulses in air”, Opt. Comm. **210**, 329–341, 2002
10. P. Rairoux, H. Schillinger, S. Niedermeier, M. Rodriguez, F. Ronneberger, R. Sauerbrey, B. Stein, D. Waite, C. Wedekind, H. Wille, L.Wöste, C. Ziener, “Remote sensing of the atmosphere using ultrashort laser pulsem”,Appl. Phys. B **71**, 573-580, 2000
11. J. Kasparian, M. Rodriguez, G. Méjean, J. Yu, E. Salmon, H. Wille, R. Bourayou, S. Frey, Y.-B. André, A. Mysyrowicz, R. Sauerbrey, J.-P. Wolf, L. Wöste, “White-Light Filaments for Atmospheric Analysis”, Science **301**, 61-64, 2003
12. H. Yang, J. Zhang, Y. Li, J. Zhang, Y. Li, Z. Chen, H. Teng, Z. Wei, and Z. Sheng, “Characteristics of self-guided laser plasma channels generated by femtosecond laser pulses in air”, Phys. Rev. **66**, 016406 1-4, 2002
13. A. Couairon, “Filamentation length of powerful laser pulses”, Appl. Phys. B **76**, 789–792, 2003
14. G. Mechain, A. Couairon, Y-B. Andre, C. D’Amico, M. Franco, B. Prade, S. Tzortzakis, A. Mysyrowicz, R, Sauerbrey, “Long range self-channeling of infrared laser pulses in air: a new propagation regime without ionization”, Appl. Phys. B, **79**, 379-382, 2004
15. S. K. Sharma, P. G. Lucey, M. Ghosh, H. W. Hubble, K. A. Horton, “Stand-off Raman spectroscopic detection of minerals on planetary surfaces”, Spectrochim. Acta A **59**, 2391-2407 (2003)
16. S. Svanberg, M. Bengtsson, G. Cecchi, A.D. Dernfalk, H. Edner, R. Grönlund, T. Johansson, M. Sjöholm, G. Somesfalean, and P. Weibring, “Remote surface characterization using laser-induced fluorescence and laser-induced break-down spectroscopy”, Innovative Laser Technologies for Material Diagnostics, Firenze, February 14, 2003
17. “Femtosecond Laser Pulsem. Principles and Experiments”, edited by C. Rulliere, Springer, 2005
18. E. Nibbering, G. Grillon, M. Franco, B. Prade und A. Mysyrowicz, “Determination of the inertial contribution to the nonlinear refractive index of air, N_2 and O_2 by use of unfocused high-intensity femtosecond laser pulses”, J. Opt. Soc. Am. B **14**, 650-660, 1997
19. L.V. Keldysh, “Ionization in the Field of a Strong Electromagnetic Wave”, Soviet Physics JETP **20**, 1307, 1965.
20. S.L. Chin, P. Lambropoulos, “Multiphoton Ionization of Atoms”, Academic Press, 1984
21. J. Kasparian, R. Sauerbrey, S.L. Chin, “The critical laser intensity of self-guided light filaments in air”, Appl. Phys. B 71, 877–879, 2000
22. W. L. Kruer, “The Physics of Laser Plasma Interactions”, Addison-Wesley, 1988
23. A. Chiron, “Numerical simulations of the nonlinear propagation of femtosecond optical pulses in gases”, Eur. Phys. J. D **6**, 383-396, 1999
24. L. Berge and A. Couairon, “Gas-Induced Solitons”, Phys. Rev. Lett. **86**, 1003-1006, 2001
25. H. R. Lange, G. Grillon, J.-F. Ripoche, M. A. Franco, B. Lamouroux, B. S. Prade, A. Mysyrowicz, E. T. J. Nibbering, A. Chiron, “Anomalous long-range propagation of femtosecond laser pulses through air: moving focus or pulse self-guiding?”, Opt. Lett. **23**, 120-122, 1998
26. N. Aközbek, C. M. Bowden, A. Talebpour, S. L. Chin, “Femtosecond pulse propagation in air: Variational analysis”,Physical Review E **61**, 4540-4549, 2000
27. L. Berge “Multiple Filamentation of Terawatt Laser Pulses in Air”, Phys. Rev. Lett. **92**, 225002 1-4, 2004
28. L. Berge, Cl. Gouedard, J. Schjødt-Eriksen, and H.Ward, Physica (Amsterdam) **176D**, 181, 2003
29. H. D. Ladouceur, A. P. Baronavski, D. Lohrmann, P. W. Grounds, and P. G. Girardi, “Electrical conductivity of a femtosecond laser generated plasma channel in air”, Opt. Commun. **189**, 107-111, 2001
30. H. R. Lange, A. Chiron, J.-F. Ripoche, A. Mysyrowicz, P. Breger, and P. Agostini, „High-Order Harmonic Generation and Quasiphase Matching in Xenon Using Self-Guided Femtosecond Pulsem”, Phys. Rev. Lett. **81**, 1611, 1998

31. J. Kasparian, R. Sauerbrey, D. Mondelain, S. Niedermeier, J. Yu, J.-P. Wolf, Y.-B. André, M. Franco, B. Prade, S. Tzortzakis, A. Mysyrowicz, M. Rodriguez, H. Wille, and L. Wöste, "Infrared extension of the supercontinuum generated by femtosecond terawatt laser pulses propagating in the atmosphere", Opt. Lett. **25**, 1397-1399, 2000
32. E. T. J. Nibbering, P. F. Curley, G. Grillon, B. S. Prade, M. A. Franco, F. Salin, A. Mysyrowicz, "Conical emission from self-guided femtosecond pulses in air", Opt. Lett. **21**, 62-64, 1996
33. S. Tzortzakis, B. Prade, M. Franco, A. Mysurowicz, "Time-evolution of the plasma channel at the trail of the self-guided IR feomtosecond laser pulse in air", Opt. Com. **181**, 123-127, 2000
34. A. Couairon and L. Berge, "Light Filaments in Air for Ultraviolet and Infrared Wavelengths", Phys. Rev. Lett. **88**, 35003 1-4, 2002
35. H. Wille, M. Rodriguez, J. Kasparian, D. Mondelain, J. Yu, A. Mysyrowicz, R. Sauerbrey, J.-P. Wolf, and L. Wöste, "Teramobile: a Mobile Femtosecond-Terawatt Laser and Detection System", Eur. Phys. J.: Appl. Phys. **20**, 183-190, 2002
36. P. Rohwetter, K. Stelmaszczyk, L. Wöste, R. Ackermann, G. Méjean, E. Salmon, J. Kasparian, J. Yu and J-P. Wolf, "Filament-induced remote ablation for long range LIBS operation", to be published in Spectrochim. Acta B
37. S. M. Angel, D. N. Stratus, K. L. Eland, T. Lai, M. A. Berg, Jass. M. Gold, "LIBS using dual- and ultra-short laser pulses", Fresenius J Anal Chem **369,** 320–327, 2001
38. P. Rohwetter, J. Yu, G. Méjean, K. Stelmaszczyk, E. Salmon, J. Kasparian, J.-P. Wolf, and L. Wöste "Remote LIBS with ultra-short pulses: characteristics in picosecond and femtosecond regimes", J. Anal. At. Spectrom. **19**, 437-444, 2004
39. S. Mao, X. Mao, R. Greif, and E. Russo, "Initiation of an early-stage plasma during picosecond laser ablation of solids", App. Phys. Lett. **70**, 2464-2466, 2000
40. S. Zamith, J. Degert, S. Stock, B. de Beauvoir, "Observation of Coherent Transients in Ultrashort Chirped Excitation of an Undamped Two-Level System", Phys. Rev. Lett. **87**, 033001 1-4, 2001
41. Ch. J. Bardeen, V. V. Yakovlev, K. R. Wilson, S. D. Carpenter, P. M. Weber and W. S. Warrend, "Feedback quantum control of molecular electronic population transfer", Chem. Phys. Lett. **280**, 151-158, 1997
42. "Laser Ablation and Desorption", edited by J. C. Miller and R. F. Haglund, Jr., Academic, New York, 1998
43. K. Stelmaszczyk, P. Rohwetter, G. Méjean, J. Yu, E. Salmon, J. Kasparian, R. Ackermann, J-P. Wolf, L. Wöste, "Long-distance remote laser-induced breakdown spectroscopy using filamentation in air", Appl. Phys. Lett., **18**, 3977-3979, 2004
44. J. C. Owens, "Optical refractive index of air: dependence on pressure, temperature, and composition", Appl. Opt., **6**, 51–59, 1967
45. S. Palanco , S. Conesa and J. J. Laserna, "Analytical control of liquid steel in an induction melting furnace using a remote laser induced plasma spectrometer", J. Anal. At. Spectrom. **19**, 462 – 467, 2004
46. H. Nishioka, W. Odajima, K. Ueda, and H. Takuma, "Ultrabroadband flat continuum generation in multichannel propagation of terrawatt Ti:sapphire laser pulses". Opt. Lett. **20**, 2505-2507, 1995